Coherent enhancement of back-scattered radiation in a randomly inhomogeneous medium: the diffusion approximation

Yu. N. Barabanenkov and V. D. Ozrin

All-Union Center for Scientific Surface and Vacuum Studies
(Submitted 29 October 1987)
Zh. Eksp. Teor. Fiz. **94**, 56–64 (June 1988)

We discuss the angular features contributed by cyclic diagrams to the multiply-scattered light intensity in a bounded randomly inhomogeneous medium occupying a three-dimensional semi-infinite space with a plane boundary. Ignoring wave polarization effects, the cyclic-diagram contribution may be expressed in terms of the Green's function for the transport equation governing the radiation leaving the medium. This Green's function can be calculated in the diffusion approximation, with boundary conditions specified for the normal logarithmic derivative of the radiation intensity. Our main result is a demonstration of the existence, within the scope of the assumptions, of three regimes for the cyclic-diagram contribution to the radiative intensity as a function of the angle ϑ measured from the backwards direction. These three regimes are described for a number of different values of the mean cosine μ of the scattering angle from an effective inhomogeneity in the medium. All three cyclic-diagram regimes have been confirmed experimentally, with a positive triangular peak at $\vartheta = 0$. If $\mu < \mu_{\rm cr} = \frac{1}{3}$, the cyclic-diagram contribution decreases with increasing ϑ, tending to zero as ϑ^{-2}. For $\mu = \mu_{\rm cr}$, this contribution goes to zero as ϑ^{-3}. Finally, for $\mu > \mu_{\rm cr}$, the cyclic-diagram contribution passes through zero as ϑ increases, reaches a negative minimum, and ultimately tends to zero through negative values as $-\vartheta^{-2}$.

1. INTRODUCTION

The coherent enhancement of back-scattered electromagnetic or acoustic waves in a randomly inhomogeneous medium is presently of great interest by virtue of its importance in the general theory of multiple scattering. The effect was first noticed in a theoretical treatment of back-scattered electromagnetic waves in a turbulent plasma in the second Born approximation,[1] and to all orders of perturbation theory among pairwise correlated electrons in a plasma.[2] The enhancement of back-scattered radiation superposed on a background of multiply forward-scattered radiation was demonstrated in Ref. 3 for the special case of a turbulent medium with large-scale inhomogeneities. This result was subsequently interpreted[4–6] to be the physical result of a single wave traversing the same large-scale inhomogeneities twice. Barabanenkov[7] established the fact that the enhancement of back-scattered radiation is independent of the statistical properties of the fluctuations in the dielectric constant of either a continuous medium or one consisting of arbitrary size scattering centers in a discrete medium, and developed a method based on radiative transfer theory for computing the angular distribution of amplified scattered intensity close to the backward direction.[1)]

Backward scattering enhancement is characteristic of a variety of wave fields and a number of randomly inhomogeneous media for which the Green's function of the field is time-reversal invariant.[9] An analogous phenomenon in the theory of mixture conductivity[10] is known as weak localization. The phenomenon is manifested as a discrepancy between the conductivity of a disordered system and the value predicted by classical kinetic theory.[11,13] Optical and acoustical experiments enable one to detect weak localization of waves through enhancement of the back-scattering of light in a dense aqueous suspension of submicron latex or polystyrene particles[13–16] or in a disordered solid medium containing submicron particles,[17,18] and through back-scattering of sound in an ensemble of hard scatterers.[19] In the optical experiments, one measures the angular distribution of the scattered luminous intensity from the suspension or the disordered solid medium close to the backward direction; the dependence of the measured angular distributions on the polarization of the incident and scattered light is then investigated. A theoretical interpretation of the measurements is given in Refs. 20–24, and is based on a calculation of the contribution of cyclic diagrams,[7] also known as maximally connected or fan diagrams,[10,11,25] to the lumimous intensity of the radiation scattered by the medium. In this calculation, the contribution of a second-order cyclic diagram can be computed directly,[20] while the sum of higher-order contributions from such diagrams[21–24] can be obtained[7] using a diffusion approximation. Note that the proposed theoretical interpretation of the measurements is limited to a model consisting of point scatterers (effective inhomogeneities). However, taking the experiment described in Ref. 14 as an example, the size of the polystyrene particles in aqueous suspension is comparable to the wavelength of light. In comparing their calculations with the results of that experiment, Akkermans *et al.*[21] had to replace the extinction length for light in their final formula with the transport length for extinction.

In the present paper, we calculate the contribution made by cyclic diagrams to the luminous intensity of radiation scattered by a finite, randomly inhomogenous medium with an arbitrary ratio between the effective inhomogeneity scale and the wavelength. For simplicity, we solve this problem by starting with the scalar Helmholtz wave equation, which is in satisfactory agreement with the optical experiments[14–18] if the incident and scattered radiation have the same polarization. The contribution of the cyclic diagrams is represented as a Fourier transform of the solution of the

 0038-5646/88/061117-05$04.00

transfer equation along the boundary of the medium, corresponding physically to the scattering function of a collimated beam of finite width. Close to the backward direction, the main contribution to the transform comes from well-separated entry and exit beams. This forms the basis for use of the diffusion approximation in solving the radiative transfer equation in an optically thick medium. The boundary conditions for the diffusion equation are formulated to make use of the requirement that there be no incoming scattered radiation at the boundary of the medium.[26] We discuss other versions of the boundary conditions, specifically those associated with the vanishing of the radiative intensity at the effective boundary of the medium,[7,9,21–24] as well as those derived from an exact solution of the transport equation for a semi-infinite space. We perform actual calculations for a medium with such a geometry. We show that for sufficiently large-scale inhomogeneities, the contribution made by cyclic diagrams is responsible for the enhancement of "almost backward" scattering ($0 \leqslant |\vartheta| \leqslant \vartheta_0$), and the diminution of scattering in the adjoining cone ($\vartheta_0 \leqslant |\vartheta| \leqslant 1$). This result is consistent with the usual interference-pattern approach and with the prediction made by Vinogradov *et al.*[5]

2. THE CONTRIBUTION OF CYCLIC DIAGRAMS TO THE SCATTERED LUMINOUS INTENSITY

Let a monochromatic plane wave $\exp(ik_0 s_0 \mathbf{r})$ with wave number k_0 and directional unit vector s_0 be incident upon a randomly inhomogeneous medium. The correlation function of the field scattered by the medium will be governed by the incoherent scattering operator[7] U, which obeys the relation

$$\langle G(\mathbf{r}_1,\mathbf{r}_1')G^*(\mathbf{r}_2,\mathbf{r}_2')\rangle-\langle G(\mathbf{r}_1,\mathbf{r}_1')\rangle\langle G^*(\mathbf{r}_2,\mathbf{r}_2')\rangle$$
$$=\int d^3r_3\,d^3r_3'\,d^3r_4\,d^3r_4'\,G_0(|\mathbf{r}_1-\mathbf{r}_3|)G_0^*(|\mathbf{r}_2-\mathbf{r}_4|)$$
$$\cdot U(\mathbf{r}_3,\mathbf{r}_3';\mathbf{r}_4,\mathbf{r}_4')G_0(|\mathbf{r}_3'-\mathbf{r}_1'|)G_0^*(|\mathbf{r}_4'-\mathbf{r}_2'|). \tag{1}$$

Here $G(\mathbf{r},\mathbf{r}')$ is the Green's function for the wave field, $G_0(r)=\exp(ik_0r)/(-4\pi r)$ is its value in a homogeneous medium, $\langle\ldots\rangle$ represents an ensemble average, and the asterisk denotes complex conjugation. We introduce the Fourier transform

$$\tilde{U}(\mathbf{p},\mathbf{p}';\mathbf{q},\mathbf{q}')=\int d^3r_1\,d^3r_1'\,d^3r_2\,d^3r_2'\,U(\mathbf{r}_1,\mathbf{r}_1';\mathbf{r}_2,\mathbf{r}_2')$$
$$\cdot\exp[-i(\mathbf{p}\mathbf{r}_1-\mathbf{p}'\mathbf{r}_1')+i(\mathbf{q}\mathbf{r}_2-\mathbf{q}'\mathbf{r}_2')] \tag{2}$$

and denote by $\tilde{U}(\mathbf{s},\mathbf{s}')$ its diagonal elements on the k_0^2 surface,

$$\tilde{U}(\mathbf{s},\mathbf{s}')=\tilde{U}(k_0\mathbf{s},k_0\mathbf{s}';k_0\mathbf{s},k_0\mathbf{s}'), \tag{3}$$

where $\mathbf{s}$ and $\mathbf{s}'$ are unit vectors. In addition, we denote by $\Pi_{\rm inc}(\mathbf{r})$ the mean energy flux vector obtained by subtracting off the energy flux vector of the mean field. According to (1), in the Fraunhofer zone of the bulk medium,

$$\mathbf{\Pi}_{\rm inc}(\mathbf{r})\,|_{r\to\infty}=\frac{k_0\mathbf{s}}{(4\pi)^2r^2}\tilde{U}(\mathbf{s},\mathbf{s}_0),\qquad \mathbf{s}=\frac{\mathbf{r}}{r}. \tag{4}$$

This signifies that the quantity $\tilde{U}(\mathbf{s},\mathbf{s}')$ makes its appearance as a differential cross section for incoherent (or partially coherent) scattering by the medium.[7] Besides the Fourier transform (2) of the kernel of the incoherent scattering operator with respect to its four arguments, it is also convenient to employ its Fourier transform with respect to the two differences $(\mathbf{r}_1-\mathbf{r}_2)$ and $(\mathbf{r}_1'-\mathbf{r}_2')$, taking

$$U(\mathbf{R},\mathbf{p};\mathbf{R}',\mathbf{p}')$$
$$=\int d^3r\,d^3r'\,\exp(-i\mathbf{p}\mathbf{r}+i\mathbf{p}'\mathbf{r}')\,U\Big(\mathbf{R}+\frac{\mathbf{r}}{2},\,\mathbf{R}-\frac{\mathbf{r}}{2};$$
$$\mathbf{R}'+\frac{\mathbf{r}'}{2},\,\mathbf{R}'-\frac{\mathbf{r}'}{2}\Big). \tag{5}$$

In particular we find that

$$\tilde{U}(\mathbf{s},\mathbf{s}')=\int d^3R\,d^3R'\,U(\mathbf{R},k_0\mathbf{s};\mathbf{R}',k_0\mathbf{s}').$$

Let us now suppose that the medium occupies a plane layer $0<z<L$. Within this layer, the kernel of the incoherent scattering operator is translationally invariant in any plane perpendicular to the z-axis. The right-hand side of (5) is then proportional to the cross-sectional area Σ of the layer, which enables us to put

$$I(\mathbf{s})=\frac{\tilde{u}(\mathbf{s},\mathbf{s}_0)}{|s_z|},\qquad \tilde{u}(\mathbf{s},\mathbf{s}_0)=\frac{\tilde{U}(\mathbf{s},\mathbf{s}_0)}{(4\pi)^2\Sigma}. \tag{7}$$

Of these two dimensionless quantities, the first is the luminous intensity of radiation scattered outside the layer,[7] and the second is essentially the albedo in a given scattering direction.[9,21]

The integrand on the right-hand side of (6) can be found by solving the radiation transport equation. To check that this is the case, we first denote the mean bilinear combination of Green's functions $\langle G\times G^*\rangle$ and the bilinear combinations $\langle G\rangle\times\langle G^*\rangle$ and $G_0\times G_0^*$ by Φ, Φ_0, and Φ_{00}, respectively. The mean Green's function $\langle G\rangle$ satisfies the Dyson (D) equation with mass operator $M(\mathbf{r},\mathbf{r}')$. The quantity Φ is a solution of the Bethe-Salpeter (B-S) equation,

$$\Phi=\Phi_0+\Phi_0K\Phi, \tag{8}$$

with intensity operator $K(\mathbf{r}_1,\mathbf{r}_1';\mathbf{r}_2,\mathbf{r}_2')$; for conciseness in (8), we have omitted arguments and convolution integrals of the type (1). The Feynman diagrams contributing to the kernels M and K may be decomposed into single-group and multigroup diagrams.[7] The single-group diagrams are constructed from scatterers belonging to a single correlation group which are joined by a single correlation function. The contribution they make to the kernels M and K falls off in the same way as the correlation functions of the scatterers as their arguments become more widely spaced.[2)] Multigroup diagrams, containing several scatterer correlation groups, contribute to M and K in a manner that falls off with argument spacing as some power of the Green's function. Multigroup diagrams include cyclic diagrams.

In the kernels M and K, let us first retain only single-group diagrams: $M\to M_1$, $K\to K_1$. We then make use of the Fraunhofer approximation[27] in solving the D and B-S equations, taking the effective inhomogeneities in the medium to be in the Fraunhofer zone relative to one another and to the source and observation points.

In the Fraunhofer approximation, the mean Green's function can be written out with the aid of the effective complex wave number. Take the Fourier transform of the kernels

Φ, Φ_0, and Φ_{00} with respect to coordinate differences of the type (5), introducing a factor $(2\pi)^{-6}$ on the right-hand side. In the Fraunhofer approximation, these spectral densities are concentrated about p and p' on the k_0^2-surface[28],

$$(\Phi, \Phi_0, \Phi_{00})(\mathbf{R}, \mathbf{p}; \mathbf{R}', \mathbf{p}') = (F, F_0, F_{00})(\mathbf{R}, \mathbf{s}; \mathbf{R}', \mathbf{s}') k_0^{-4}\delta(p-k_0)\delta(p'-k_0), \quad \mathbf{s}=\mathbf{p}/p, \quad \mathbf{s}'=\mathbf{p}'/p'. \tag{9}$$

The B-S equation (8) then reduces to the radiative transfer equation:

$$(\mathbf{s}\nabla_R+d^{-1})F(\mathbf{R},\mathbf{s};\mathbf{R}',\mathbf{s}')=(4\pi)^{-2}\delta^{(3)}(R-R')\delta^{(2)}(s-s') + \int d^2s''\, W(\mathbf{s},\mathbf{s}'')F(\mathbf{R},\mathbf{s}'';\mathbf{R}',\mathbf{s}'), \tag{10}$$

$$W(\mathbf{s},\mathbf{s}')=(4\pi)^{-2}\int d^3R\, d^3r\, d^3r' \exp[-ik_0(\mathbf{sr}-\mathbf{s}'\mathbf{r}')] \cdot K_1\left(\mathbf{R}+\frac{\mathbf{r}}{2}, \mathbf{R}-\frac{\mathbf{r}}{2}; \mathbf{R}'+\frac{\mathbf{r}'}{2}, \mathbf{R}'-\frac{\mathbf{r}'}{2}\right),$$
$$d^{-1}=\int d^2s\, W(\mathbf{s},\mathbf{s}'). \tag{11}$$

Barabanenkov *et al.*[29] have given an explicit expression for the scattering coefficient $W(\mathbf{s}, \mathbf{s}')$ in terms of the plane-wave scattering amplitude for clusters with $N \geqslant 1$ scatterers, and in terms of cluster correlation functions. The kernel F_0 satisfies Eq. (10) without the term containing the scattering coefficient; if we also discard the term with the extinction coefficient d^{-1}, we obtain the equation for F_{00}. Substituting (9) into (1) gives

$$F-F_0 \equiv F_s = F_{00}U_1F_{00}. \tag{12}$$

The subscript 1 here indicates the single-group approximation; arguments R and $\mathbf{s}$ have been omitted, as well as convolution integrals over these arguments. The operator $(4\pi)^2\mathbf{s}\nabla_R$, which functions as the inverse of F_{00}, enables one to solve Eq. (12) for U_1 (Ref. 7). Substituting the result into (6) and (7), changing notation $I \to I_1$, and performing some rearrangement, we have

$$I_1(\mathbf{s})=(4\pi)^2 s_{0z}\int d^2R_\perp F_s(\mathbf{R}_\perp;0,\mathbf{s};0,\mathbf{s}_0), \quad s_{0z}>0, \quad s_z<0. \tag{13}$$

The solution of the transport equation (10) without the source term defined by the identity (12) may be written as $F_s(\mathbf{R}_\perp - \mathbf{R}_\perp'; z,\mathbf{s}; z', \mathbf{s}')$, where $\mathbf{R}_\perp$ and $\mathbf{R}_\perp'$ are the components of $\mathbf{R}$ and $\mathbf{R}'$ perpendicular to the z-axis. In the integrand of Eq. (13), this solution characterizes scattering by the medium of a narrow beam incident upon the $z = 0$ surface at the point $\mathbf{R}_\perp' = 0$, $z' = 0$ in the direction $\mathbf{s}' = \mathbf{s}_0$, and leaving the same surface at the point $\mathbf{R}_\perp$, $z = 0$ in the direction $\mathbf{s}$. Making use of the transport equation, (13) may be brought to the form

$$I_1=I^{(1)}+I_1',$$
$$I_1'(\mathbf{s})=\frac{2\pi(4\pi)^2}{|s_z|}\int_0^\infty R_\perp dR_\perp \int_0^L\int dz\, dz' \exp(-\alpha z-\alpha' z') \cdot \iint d^2s'\, d^2s''\, W(\mathbf{s},\mathbf{s}')F(R_\perp; z,\mathbf{s}'; z',\mathbf{s}'')W(\mathbf{s}'',\mathbf{s}_0),$$
$$\alpha=(|s_z|d)^{-1}, \quad \alpha'=(s_{0z}d)^{-1}. \tag{14}$$

This representation of the luminous intensity of the scattered radiation, where $I^{(1)}$ is associated with simple scattering, is less transparent than (13), but it is computationally more convenient, as it contains the complete solution of the transport equation (10) right in the integrand.

In the present approach to solving the Dyson and Bethe-Salpeter equations, when their kernels retain only single-group diagrams, the latter reduces to the transport equation. For a narrow scattering cone in the backwards direction ($s \approx -s_0$), however, it has been found[7,8] that the single-group approximation is not sufficient, and the operator must also incorporate the contributions of cyclic diagrams, whose sum we denote by K_c. Perturbation theory gives the solution of the Bethe-Salpeter equation with intensity operator $K_1 + K_c$ as $U \approx U_1 + U_c$, where U_c is the contribution of cyclic diagrams to the incoherent scattering operator. Based on the reciprocity relations between the kernels M_1 and K_1, we obtain[7]

$$\tilde{U}_c(\mathbf{s}, \mathbf{s}_0)=\mathrm{Re}\,\tilde{U}_1'(-k_0\mathbf{s}_0, -k_0\mathbf{s}; k_0\mathbf{s}, k_0\mathbf{s}_0), \tag{15}$$

where U_1' is the incoherent scattering operator U_1 minus its value in the single-scattering approximation. Using (5), we can reduce this equation to the form

$$\tilde{U}_c(\mathbf{s},\mathbf{s}_0)=\int d^3R\, d^3R' \cos[k_0(\mathbf{s}+\mathbf{s}_0)(\mathbf{R}-\mathbf{R}')] \cdot U_1'(\mathbf{R}, -\varkappa\mathbf{s}_1; \mathbf{R}', \varkappa\mathbf{s}_1),$$
$$\varkappa=k_0|\mathbf{s}_0-\mathbf{s}|/2, \quad \mathbf{s}_1=(\mathbf{s}_0-\mathbf{s})/|\mathbf{s}_0-\mathbf{s}|. \tag{16}$$

The quantity U_1' here is analogous to the expression in the integrand of (6), and it can be determined by solving the transport equation. Successively substituting Eqs. (16) into (7), with $I \to I_1$, we have

$$I_c(\mathbf{s}) \approx (4\pi)^2(s_{1z}^2/|s_z|)\int d^2R_\perp \cos[k_0(\mathbf{s}+\mathbf{s}_0)\mathbf{R}_\perp] \cdot F_s'(\mathbf{R}_\perp; 0, -\mathbf{s}_1; 0, \mathbf{s}_1). \tag{17}$$

The prime on F_s' signifies that the single-scattering contribution has been taken out of F_s. Just as (13) is transformed into (14), the contribution of cyclic diagrams to the scattered luminous intensity (17) may be brought to the form

$$I_c(\mathbf{s})=\frac{2\pi(4\pi)^2}{|s_z|}\int_0^\infty R_\perp dR_\perp \int_0^L\int dz\, dz'\, J_0(pR_\perp) \cdot \exp(-\beta z-\beta^* z') \cdot \iint d^2s'\, d^2s''\, W(-\mathbf{s}_1,\mathbf{s}')F(R_\perp; z,\mathbf{s}'; z',\mathbf{s}'')W(\mathbf{s}'',\mathbf{s}_1),$$
$$\beta=(s_{1z}d)^{-1}-ik_0(s_{0z}+s_z), \quad p=k_0|\mathbf{s}_{0\perp}+\mathbf{s}_\perp|. \tag{18}$$

If we restrict our attention in the kernel M to single-group diagrams, and in the kernel K to single-group and cyclic diagrams, then the total scattered luminous intensity will be

$$I \approx I^{(1)}+I', \quad I'=I_1'+I_c. \tag{19}$$

It is clear from (14) and (18) that when $\mathbf{s} = -\mathbf{s}_0$, $I_1'(\mathbf{s})$ and $I_c(\mathbf{s})$ will have identical values, which is a manifestation of back-scattering enhancement. As the scattering deviates from the backwards direction $I_c(\mathbf{s})$ should decrease, due to oscillations in the Bessel function $J_0(pR_\perp)$ appearing in the integrand in Eq. (18). The specific nature of this decrease will be discussed in the following sections.

3. DIFFUSION APPROXIMATION

When the parameter p is small, the main contribution to the integral (18) comes from large $R_\perp$. It is natural then to make use of the diffusion approximation[26] to solve the transport equation (10), with

$$F(\mathbf{R}_\perp-\mathbf{R}_\perp'; z, \mathbf{s}; z', \mathbf{s}')$$
$$=(4\pi)^{-2}[1-3D(\mathbf{s}\nabla-\mathbf{s}'\nabla')]F(\mathbf{R}_\perp-\mathbf{R}_\perp'; z, z'). \qquad (20)$$

Here D is the diffusion constant

$$D=\frac{d}{3(1-\mu)}, \qquad \mu=d\int d^2s(\mathbf{s}\mathbf{s}')W(\mathbf{s},\mathbf{s}'), \qquad (21)$$

where μ is the mean of the cosine of the scattering angle for a plane wave scattering from an inhomogeneity in the medium. The function $F(\mathbf{R}_\perp; z, z')$ satisfies the equation

$$\Delta F(\mathbf{R}_\perp-\mathbf{R}_\perp'; z, z')=-(4\pi D)^{-1}\delta^{(3)}(\mathbf{R}-\mathbf{R}'), \qquad (22)$$

with boundary condition

$$\left[2D\gamma\frac{\partial}{\partial z}F(\mathbf{R}_\perp; z, z')-F(\mathbf{R}_\perp; z, z')\right]_{z=0}=0; \qquad (23)$$

the sign of the second term is reversed at the other surface, $z=L$. The parameter γ is introduced here to account for different boundary conditions: $\gamma=1$ when the total inward-directed flux at the surface $z=0$ tends to zero, for an isotropic source located at z', with $0<z'<L$; $\gamma=\frac{3}{4}$ is obtained when one considers the behavior of the solution to Eq. (10) in integral form in the diffusion limit $R_\perp, z'\gg d$ for the near-boundary region $0\leqslant z\lesssim d$, with an isotropic scattering coefficient; for $\gamma=z_0/2D$, the asymptotic solution of (22), (23), where $z_0\approx 0.71d$ is the extrapolated length in the Milne problem,[26] is of the same form as in the case of the boundary condition $F(R_\perp; z=-z_0, z')=0$ used in Refs. 7,9, and 21–24; finally, one of the authors (V.D.O.) has obtained an exact solution to (10) for a semi-infinite space ($L\to\infty$), which for $R_\perp\to\infty$ and $z, z'\sim d$ behaves in the same way as the asymptotic solution of (22), (23) when $\gamma=\bar{z}_0/2D$, where $\bar{z}_0/d$ is a number for which a crude estimate is $(4z_0-d)/3<\bar{z}_0<z_0$.

We should also point out that in contrast to the problem in an unbounded medium, the gradient terms in (20) are not small in comparison with F in the near-boundary region $0\leqslant z, z'\lesssim d$, which in fact provides the main contribution to the integral (18). The problem posed for the Laplace equation (22) is solved by Fourier transformation in the transverse coordinates. Using the resulting solution, the quadratures of (18) are calcualted in final form.

We can also generate the value of (14) in the diffusion approximation (20)–(23). For a semi-infinite medium, we find that

$$I_1'(\mathbf{s})=\frac{\gamma s_{0z}}{2\pi}\left[1+\frac{3}{2\gamma}(1+\mu)\frac{s_{0z}|s_z|}{s_{0z}+|s_z|}\right], \qquad (24)$$

$$I_c(\mathbf{s})=\frac{\gamma(s_{1z})^2}{2\pi|s_z|}\left[\frac{1-\mu-2\mu s_{1z}pd}{1-\mu+2\gamma pd/3}+\frac{3}{4\gamma}(1+\mu)s_{1z}\right]$$
$$\cdot[(1+s_{1z}pd)^2+(s_{1z}k_0d)^2(s_{0z}+s_z)^2]^{-1}. \qquad (25)$$

4. ANGULAR DEPENDENCE OF THE CONTRIBUTION FROM CYCLIC DIAGRAMS

Let us analyze these results for the simplest case, that of normal incidence at the boundary of the medium, and small angles ϑ: $s_{0z}=1, s_z=-\cos\vartheta, |\vartheta|\ll 1$. We begin by assuming that $I_1(\vartheta)\approx I_1'(0)$. Then (24) and (25) yield

$$\delta(\vartheta)=[I_1'(0)+I_c(\vartheta)]/I_1'(0)$$
$$=1+(1+q)^{-2}\left[1-\frac{2(\mu+\gamma/3)}{1+3(1+\mu)/4\gamma}\cdot\frac{q}{1-\mu+2\gamma q/3}\right],$$
$$q=k_0d|\vartheta|. \qquad (26)$$

In the limit of small q, we then obtain

$$\delta(\vartheta)\approx 2(1-q/4q_{1/2}), \qquad q\ll 1-\mu,$$
$$4q_{1/2}\approx(1-\mu)(1+2\gamma/3)3[2\gamma(1+\gamma/3)]^{-1}. \qquad (27)$$

The curve for $\delta(\vartheta)$ therefore has a triangular peak at $\vartheta=0$ with halfwidth $q_{1/2}$ at the half-power level. In the event that we have fine-scale irregularities, $\mu\ll 1$, Eq. (27) is the same as the result obtained in Ref. 21 if $\gamma=3z_0/2d$. For large-scale inhomogeneities, $1-\mu\ll 1$,

$$4q_{1/2}\approx(1-\mu)(1+2\gamma/3)3[2\gamma(1+\gamma/3)]^{-1}$$

and up to a numerical factor of order unity, the corresponding value of the angular variable $\vartheta_{1/2}$ is $(k_0\bar{d})^{-1}$, where $\bar{d}=d/(1-\mu)$ is the transport length for extinction. Overall, the behavior of $\delta(\vartheta)$ is a strong function of the mean cosine. For $\mu=\mu_{cr}=\frac{1}{3}$, it takes the form

$$\delta(\vartheta)=1+(1+q)^{-2}(1+\gamma q)^{-1}. \qquad (28)$$

For $\mu<\mu_{cr}$, δ still falls off monotonically with increasing q, but displays a different asymptotic behavior:

$$\delta(\vartheta)\approx 1+(1-3\mu)(1+\mu+4\gamma/3)^{-1}q^{-2}, \qquad q\gg 1. \qquad (29)$$

Finally, for $\mu>\mu_{cr}$, the contribution of cyclic diagrams (25) at sufficiently large scattering angles is negative, and the curve for $\delta(\vartheta)$ crosses the $\delta=1$ axis at $q=q_0$, attains a minimum at $q=q_m$, and proceeds to the asymptote (29), where $\delta<1$. The value of q_0 and a crude estimate for q at the minimum are

$$q_0=2(1-\mu)(1+3(1+\mu)/4\gamma)(3\mu-1)^{-1},$$
$$q_m=[(3+\gamma)(1-\mu)/2\gamma]^{1/2}, \qquad 1-\mu\ll 1. \qquad (30)$$

For $\gamma=1$, the three behaviorial regimes for $\delta(\vartheta)$ are illustrated in Fig. 1, where from top to bottom, the curves correspond to $\mu=0, \frac{1}{3}, \frac{2}{3}$, 0.93, 0.99, and 1. In Fig. 2, we have plotted the function (26) as applied to the experimental conditions described in Ref. 14, where $\lambda=633$ nm,

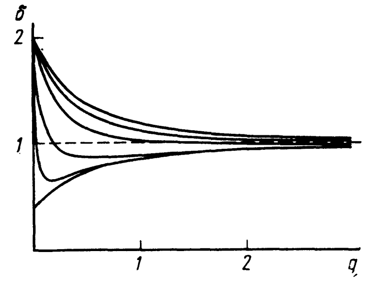

FIG. 1.

$d = 2.6\,\mu$m, and $\mu = 0.93$. If we substitute these parameters into (27) and (30), we obtain $\vartheta_{1/2} = 1.2$ mrad$(q_{1/2} = 0.03)$, $\vartheta_0 = 7.4$ mrad$(q_0 = 0.19)$, and $\vartheta_m = 15$ mrad$(q_m = 0.37)$. The experimental curve for the back-scattered intensity is given in Ref. 14 over the angular range $0 < \vartheta < 10$ mrad, and gives a conical half angle at half-maximum of $(\vartheta_{1/2})_{\rm exp} = 1.6$ mrad.

In closing, we point out that the triangular peak in the back-scattered intensity is directly related to the $F \sim R_\perp^{-3}$ asymptotic behavior of the solution of the diffusion equation (or the diffusive asymptotic behavior of the exact solution of the transport equation) as $R_\perp \to \infty$, which in turn is due to the presence of a single sharp boundary, where[21] $F \approx 0$. For a plane layer with boundary condition (23), the behavior goes asymptotically as $F \sim \exp(-bR_\perp)/R_\perp^{1/2}$, and from (14) and (18), we obtain

$$\delta(\vartheta) \approx 2 - \frac{2d}{3L}(k_0 L\vartheta)^2\left(1+\frac{2\gamma}{3}\right)^2\left(1+\frac{4\gamma}{3}\right)^{-1}, \qquad \mu = 0, \quad k_0 L|\vartheta| \ll 1. \tag{31}$$

A simplified treatment of the boundary conditions[30] yields a similar result. Equation (31) makes it clear that the narrow maximum in $\delta(\vartheta)$ has been rounded off; the finite thickness of the layer produces an analogous effect. We further note that although the diffusion approximation makes an exact calculation of the linear dependence of $\delta(\vartheta)$ possible at small $|\vartheta|$, it also lowers the maximum intensity

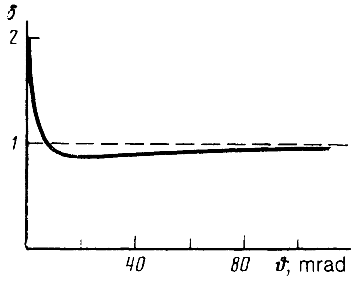

FIG. 2.

$I(0)$, which in particular contains a contribution from single scattering.

The authors are grateful to L. A. Pokrovskii, and they thank S. M. Rytov and V. I. Tatarskii for discussions of this work.

[1)] According to Refs. 2 and 7, phenomenological radiation transport theory does not take the enhancement of backwards scattering into consideration. Nevertheless specific properties of this effect can be calculated using the transport theory machinery (see also Ref. 8).

[2)] We should mention that the single-group approximation for the kernels M and K includes terms characteristic of an independent-scatterer model, which fall off with argument spacing as the potential of an isolated scatterer.

[1] R. S. Ruffine and D. A. De Wolf, J. Geophys. Res. **70**, 4313 (1965).
[2] K. M. Watson, J. Math. Phys. **10**, 688 (1969).
[3] D. A. De Wolf, Trans. IEEE **AP-19**, 254 (1971).
[4] A. G. Vinogradov and Yu. A. Kravtsov, Izv. Vyssh. Uchebn. Zaved., Radiofiz. **16**, 1055 (1973).
[5] A. G. Vinogradov, Yu. A. Kravtsov, and V. I. Tatarskii, Izv. Vyssh. Uchebn. Zaved., Rafiofiz. **16**, 1064 (1973).
[6] Yu. A. Kravtsov and A. I. Saichev, Usp. Fiz. Nauk **137**, 501 (1982) [Sov. Phys. Usp. **25**, 494 (1982)].
[7] Yu. N. Barabanenkov, Izv. Vyssh. Uchebn. Zaved., Radiofiz. **16**, 88 (1973); Usp. Fiz. Nauk, **117**, 49 (1975).
[8] L. A. Apresyan and Yu. A. Kravtsov, *The Theory of Radiative Transfer. Statistical and Wave Aspects* (in Russian), Nauka, Moscow (1984).
[9] A. A. Golubentsev, Zh. Eksp. Teor. Fiz. **86**, 47 (1984) [Sov. Phys. JETP **59**, 26 (1984).
[10] E. Abrahams, P. W. Anderson, D. C. Licciardello, and T. V. Ramakrishnan, Phys. Rev. Lett. **42**, 673 (1979); G. Bergmann, Phys. Rep. **107**, 1 (1984).
[11] L. P. Gov'kov, A. I. Larkin, and D. E. Khmel'nitskii, Pis'ma. Zh. Eksp. Teor. Fiz. **30**, 248 (1979) [JETP Lett. **30**, 228 (1979)].
[12] B. L. Altshuler, A. G. Aronov, D. E. Khmelnitskii (Khmel'nitskii), and A. I. Larkin, Quantum Theory of Solids, Mir, Moscow (1982), p. 130.
[13] Y. Kuga and A. Ishimaru, J. Opt. Soc. Am **A1**, 831 (1984).
[14] M. P. Van Albada and Ad. Lagendijk, Phys. Rev. Lett. **55**, 2692 (1985).
[15] P. E. Wolf and G. Maret, Phys. Rev. Lett. **55**, 2696 (1985).
[16] Ad. Lagendijk, M. P. Van Albada, and M. B. Van der Mark, Physica **A140**, 183 (1986).
[17] S. Etemad, R. Thompson, and M. J. Andrejco, Phys. Rev. Lett. **57**, 575 (1986).
[18] M. Kaveh, M. Rosenbluh, I. Edrei, and I. Freund, Phys. Rev. Lett. **57**, 2049 (1986).
[19] Yu. A. Kravtsov and V. V. Ryabykin, Kr. soobshcheniya po fizike, FIAN, No. 3, 37 (1987).
[20] L. Tsang and A. Ishimaru, J. Opt. Soc. Am. **A1**, 836 (1984).
[21] E. Akkermans, P. E. Wolf, and R. Maynard, Phys. Rev. Lett. **56**, 1471 (1986).
[22] M. J. Stephen and G. Cwilich, Phys. Rev. **B34**, 7564 (1986).
[23] G. Cwilich and M. J. Stephen, Phys. Rev. **B35**, 6517 (1987).
[24] R. Berkovits and M. Kaveh, J. Phys. **C20**, L181 (1987).
[25] J. S. Langer and T. Neal, Phys. Rev. Lett. **16**, 984 (1966).
[26] K. Case and P. Zweifel, *Linear Transport Theory*, Addison-Wesley, Reading, MA (1967).
[27] Yu. N. Barabenenkov and V. M. Finkel'berg, Zh. Eksp. Teor. Fiz. **53**, 978 (1967).
[28] Yu. N. Barabenenkov, Zh. Eksp. Teor. Fiz. **56**, 1262 (1969).
[29] Yu. N. Barabenenkov, V. D. Ozrin, and M. I. Kalinin, *The Asymptotic Method in the Theory of Stochastic Dynamical Systems (in Russian)*, Energoatomizdat, Moscow (1985).
[30] I. Edrei and M. Kaveh, Phys. Rev. **B35**, 6461 (1987).

Translated by M. Damashek